Lecture No. 6 -

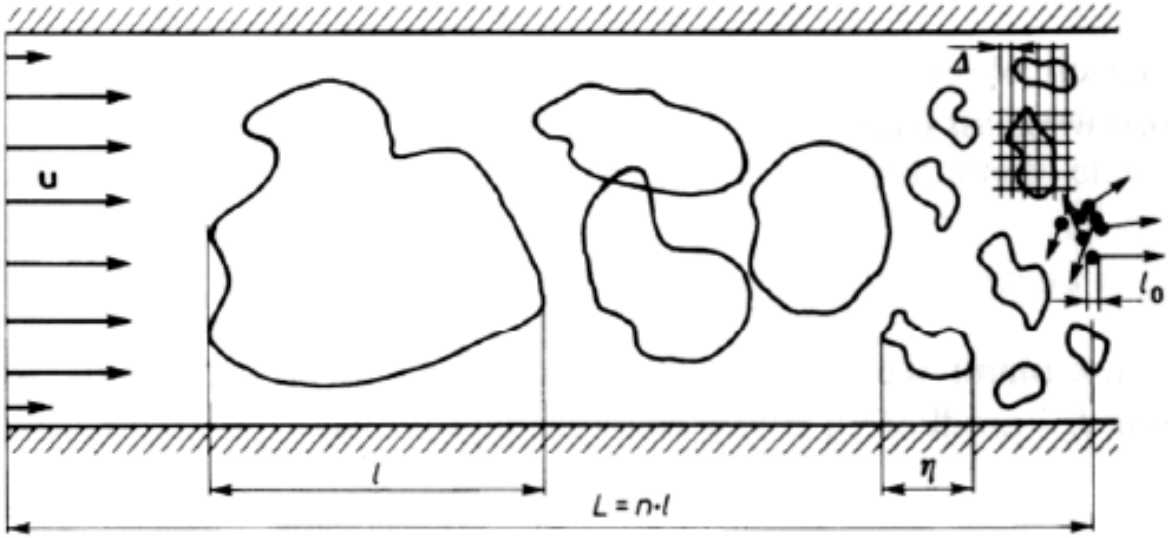

The Kolmogorov model (1941) treats **turbulence as the cascade of vortices**, transferring the energy of the fluid motion from the main flow to the molecular motion.

The largest vortices interact with the main flow and absorb its energy. Their characteristic length and velocity are of the same order as those of the main flow (high Reynolds number). It means that the inertia forces dominate and the viscosity forces are negligible. This leads to the disintegration of the vortices into smaller and faster rotating ones. The smallest vortices have Re=1 with diameter η=0.1-0.01 mm and rotational frequency10 kHz. The motion of these vortices is retarded by the viscosity forces (equal to the inertia forces), and their energy is dispersed and converted in to the internal energy (i.e. heat).

We have: $l >> \eta > l_0$ $\qquad l/\eta \approx 10^6$ $\qquad \eta/l_0 \approx 10^2$

The turbulent flow is mathematically described by the **Reynolds Equations**. Reynolds has assumed that in the turbulent flow the velocity and pressure may be expressed as sums of their mean values (or rather: slowly changing) and turbulent fluctuations, that is:

$$\bar{u} = \overline{U} + \overline{u'} \qquad p = P + p'$$

where:

$$\overline{u'} = \bar{i}u' + \bar{j}v' + \bar{k}w' \qquad \overline{U} = \bar{i}U + \bar{j}V + \bar{k}W$$

Substitution of such velocity and pressure in to the Navier-Stokes equation leads to the appearance of the new surface forces, called the **turbulent stresses:**

$$\rho\frac{DU}{Dt} = \rho f_x - \frac{\partial P}{\partial x} + \mu divgradU + \rho\left[-\frac{\partial \widetilde{u'^2}}{\partial x} - \frac{\partial \widetilde{u'v'}}{\partial y} - \frac{\partial \widetilde{u'w'}}{\partial z}\right]$$

$$\rho\frac{DV}{Dt} = \rho f_y - \frac{\partial P}{\partial y} + \mu divgradV + \rho\left[-\frac{\partial \widetilde{u'v'}}{\partial x} - \frac{\partial \widetilde{v'^2}}{\partial y} - \frac{\partial \widetilde{v'w'}}{\partial z}\right]$$

$$\rho\frac{DW}{Dt} = \rho f_z - \frac{\partial P}{\partial z} + \mu divgradW + \rho\left[-\frac{\partial \widetilde{u'w'}}{\partial x} - \frac{\partial \widetilde{v'w'}}{\partial y} - \frac{\partial \widetilde{w'^2}}{\partial z}\right]$$

Normal stresses:

$$\tau_{xx} = -\rho\widetilde{u'^2} \qquad \tau_{yy} = -\rho\widetilde{v'^2} \qquad \tau_{zz} = -\rho\widetilde{w'^2}$$

Tangential (shearing) stresses:

$$\tau_{xy} = \tau_{yx} = -\rho\widetilde{u'v'}$$

$$\tau_{xz} = \tau_{zx} = -\rho\widetilde{u'w'} \qquad \tau_{yz} = \tau_{zy} = -\rho\widetilde{v'w'}$$

The turbulent stresses, also known as Reynolds stresses, depend on the values of the velocity fluctuations, not on the fluid viscosity. It may be proved that they form a symmetrical system of stresses. They constitute the additional 6 unknowns in the system of Reynolds equations describing the turbulent motion of the fluid. In order to reduce the number of unknown sand close the system it is necessary to introduce the appropriate **models of turbulence.** The Reynolds equations are the basis of most of the contemporary commercial computer codes in the domain of the Computational Fluid Mechanics.

Chapter 19 – Boundary layers and wakes 1

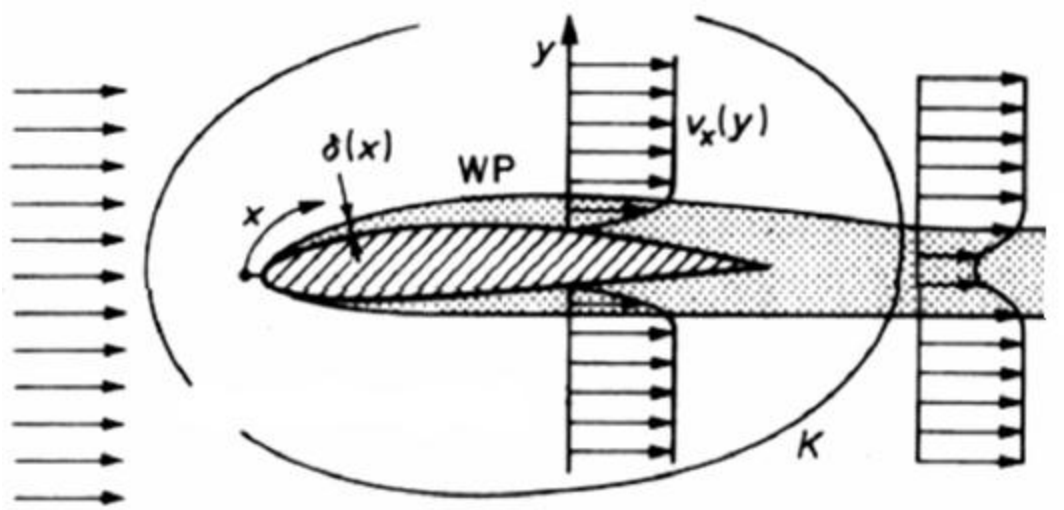

The boundary layer is the region of flow directly neighbouring on the surface of the solid body. In the boundary layer the viscosity forces play a meaningful role and the significant transverse flow velocity gradients occur. Outside the boundary layer the flow may be practically regarded as inviscid. Behind the solid body the boundary layer forms the so called wake.

The flow in the layer may be laminar or turbulent. The layer thickness δ is determined by attaining the velocity $u_\delta = 0.99 u_\infty$

A typical boundary layer on the wall of an object in contact with the flowing fluid includes the zone of laminar flow near the leading edge, the transition region and the turbulent zone. In the turbulent zone a very thin viscous sublayer is located at the wall, followed by a buffer zone further from the wall and by the dominating fully turbulent region.

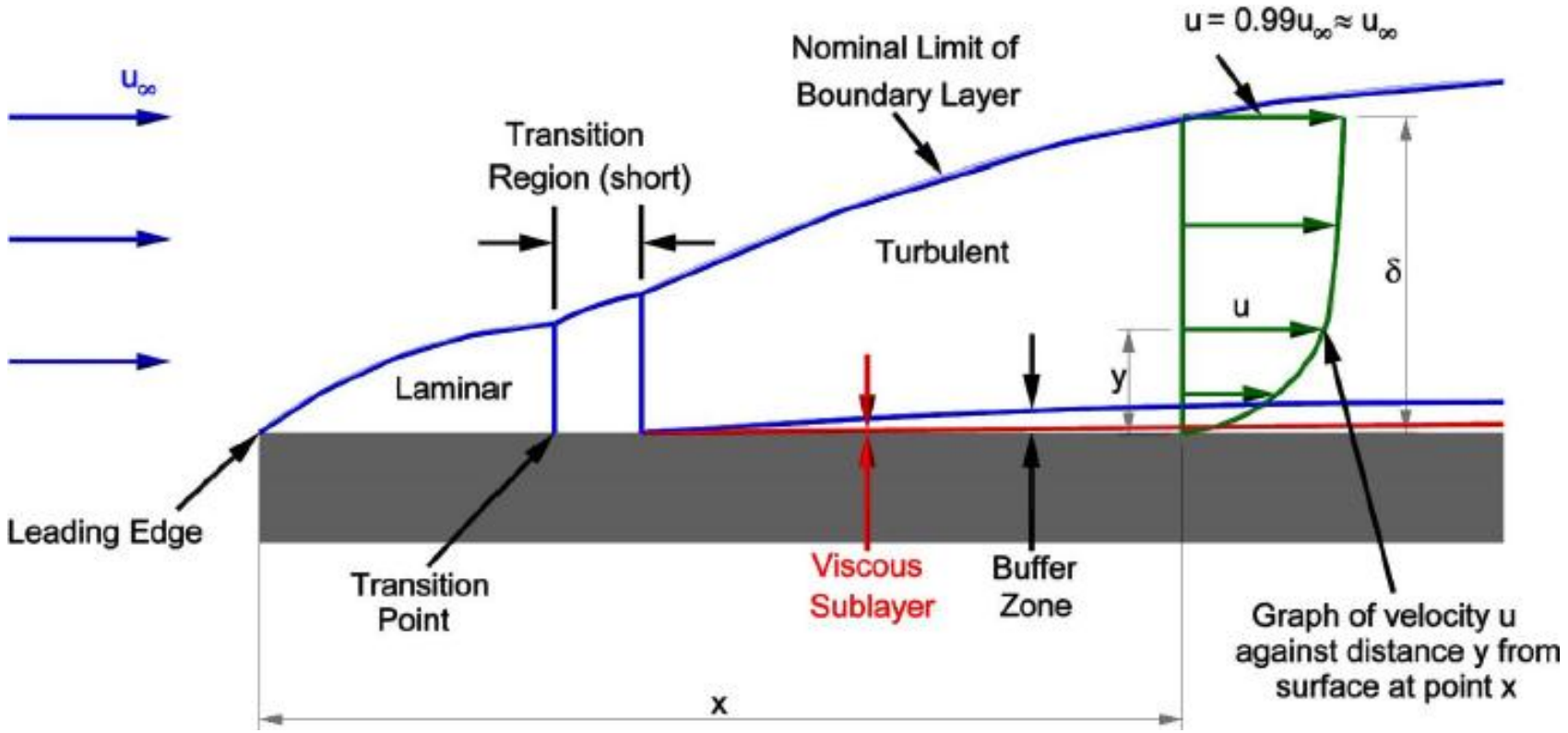

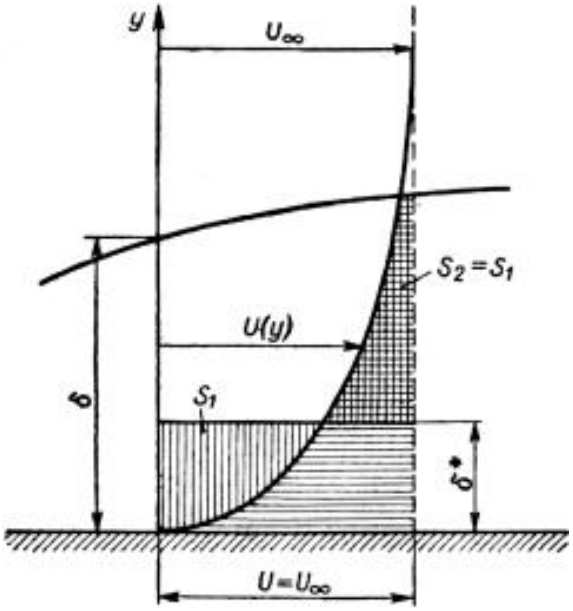

As the layer thickness δ is difficult to determine accurately, the so called displacement thickness has been introduced:

$$\delta^* = \int_0^\delta \left(1 - \frac{\rho u}{\rho_\infty u_\infty}\right) dy$$

The laminar boundary layer

The flow in a two-dimensional laminar boundary layer is described by the **Prandtl equations.** Prandtl has simplified the Navier-Stokes equation on the basis of the following assumptions:

- the layer thickness is much smaller than the wall length,
- the velocity normal to the wall is much smaller than the velocity along the outer limit of the layer.

These simplifications lead to the following equations:

$$\frac{\partial u}{\partial t}+u\frac{\partial u}{\partial x}+v\frac{\partial u}{\partial y}=-\frac{1}{\rho}\frac{\partial p}{\partial x}+\upsilon\frac{\partial^2 u}{\partial x^2}$$

direction x

$$\frac{\partial p}{\partial y}=0$$

direction y

Conclusion 1: the pressure on the wall of the solid body is equal to the pressure in the corresponding point on the outer limit of the boundary layer.

Conclusion 2: the pressure distribution on the outer limit of the boundary layer may be determined from the Bernoulli equation (in case of a steady flow).

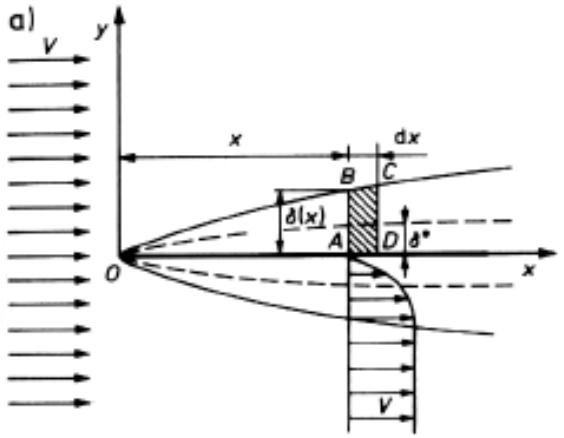

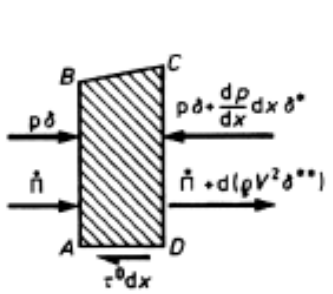

The Prandtl equations may be solved analytically for a steady flow along a flat plate (without the pressure gradient along the plate) – conf. Fig. a)

$$\frac{\partial u}{\partial x}+\frac{\partial v}{\partial y}=0$$ mass conservation equation

$$u\frac{\partial u}{\partial x}+v\frac{\partial u}{\partial y}=\upsilon\frac{\partial^2 u}{\partial y^2}$$ momentum conservation equation

Boundary conditions:

$u \to u_\infty$ at $y \to \infty$

$u = v = 0$ at $y = 0$

The solution leads to the practically useful relations:

Thickness of the laminar boundary layer on a plate:

$$\delta(x) = \frac{5x}{\sqrt{\mathrm{Re}_x}} \rightarrow \frac{\delta(x)}{x} = \frac{5}{\sqrt{\mathrm{Re}_x}}$$

where:

$$\mathrm{Re}_x = \frac{u_\infty x}{\upsilon}$$

Frictional drag coefficient on the plate surface:

$$C_f = \frac{1.328}{\sqrt{\mathrm{Re}_L}} \rightarrow R_f = C_f \cdot \frac{1}{2}\rho u_\infty^2 S$$

where:

$$\mathrm{Re}_L = \frac{u_\infty L}{\upsilon}$$

where: R_f - frictional drag of a plate of area S

Velocity profile inside the boundary layer:

$$u(y) = u_\infty \left[\frac{3}{2}\frac{y}{\delta} - \frac{1}{2}\left(\frac{y}{\delta}\right)^3 \right]$$

Moreover it may be calculated that:

$$\delta^* \approx 0.33\delta$$

Increasing of the Reynolds number leads to the losing of stability of the laminar boundary layer and to the gradual development of turbulence up to the fully developed turbulent boundary layer.

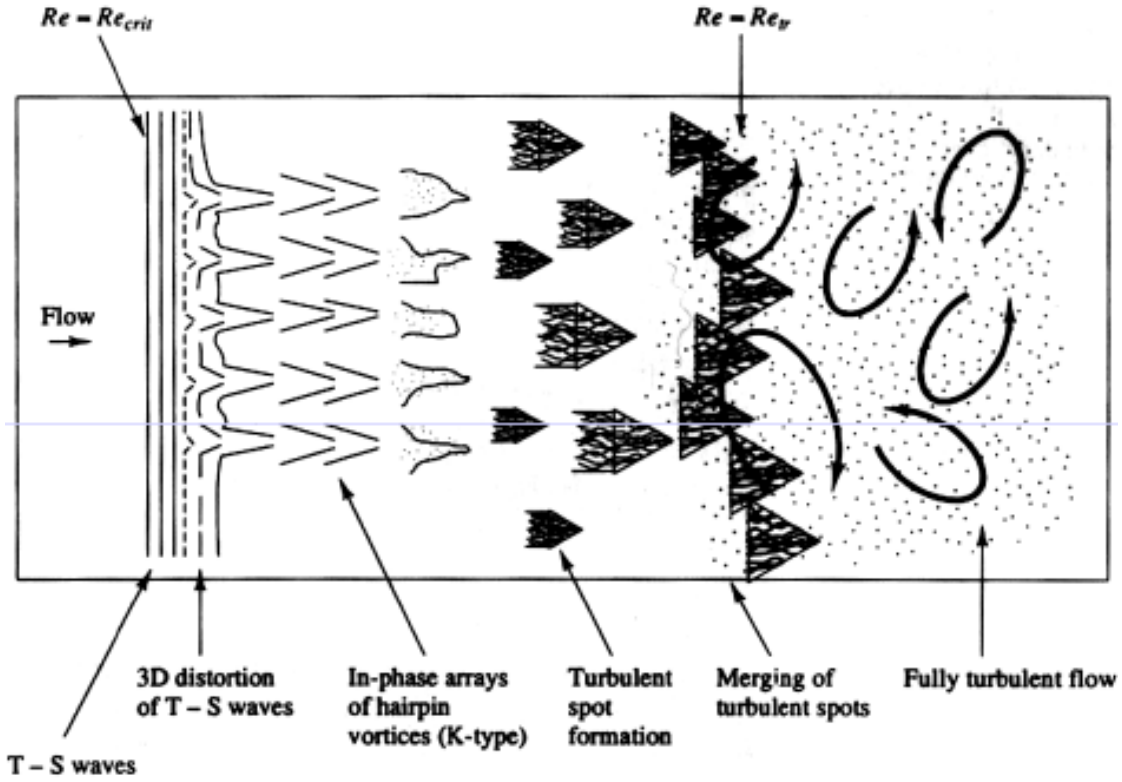

Scheme of the process of turbulization of the boundary layer.

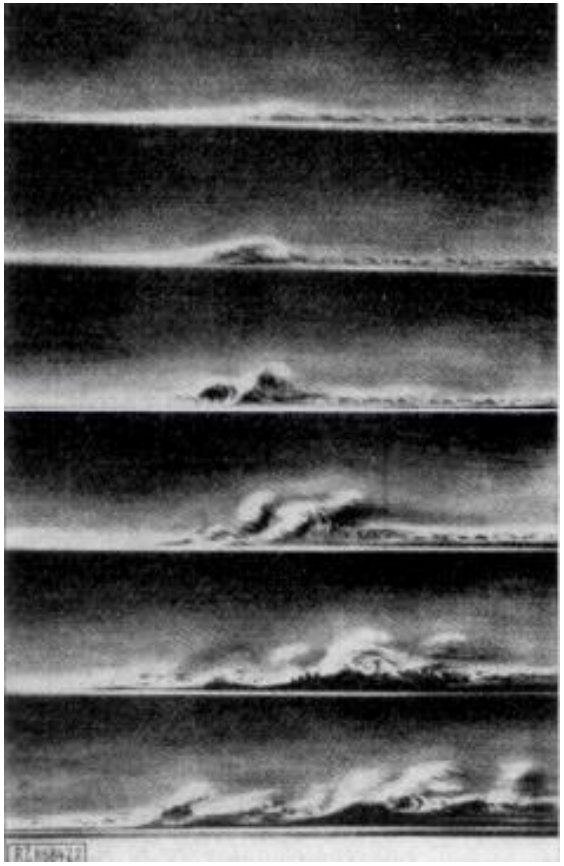

Visualization of the generation of turbulence

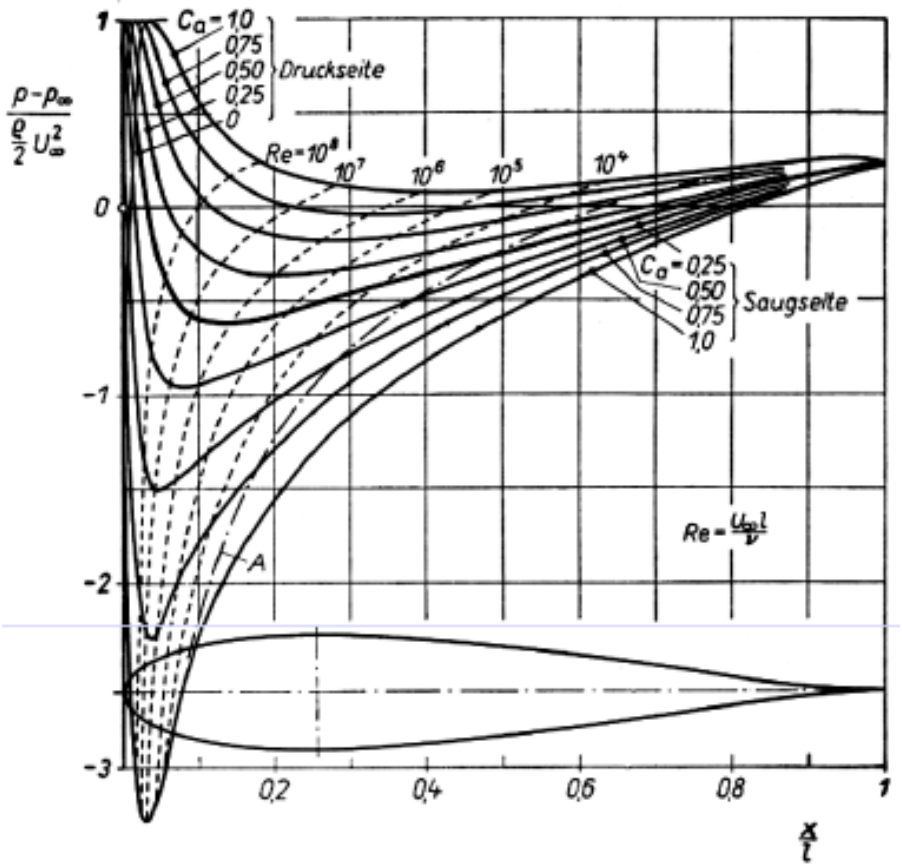

The location of the laminar turbulent
transition depends
both on the Reynolds number and on the pressure gradient along the boundary layer. The picture shows this phenomenon on an asymmetric profile set at the different angles of attack, what changes the pressure gradient. The broken lines show the location of the laminar turbulent
transition at different
values of the Reynolds number.

The **positive pressure gradient along the boundary layer** (i.e. increase of pressure in the flow direction), may lead to the so called **separation** of the boundary layer. The mechanism is explained in Fig b) on slide 4. The fluid element near the wall is retarded by the viscosity forces and pressure forces, what leads to its stopping and then inducing its motion against the direction o flow.

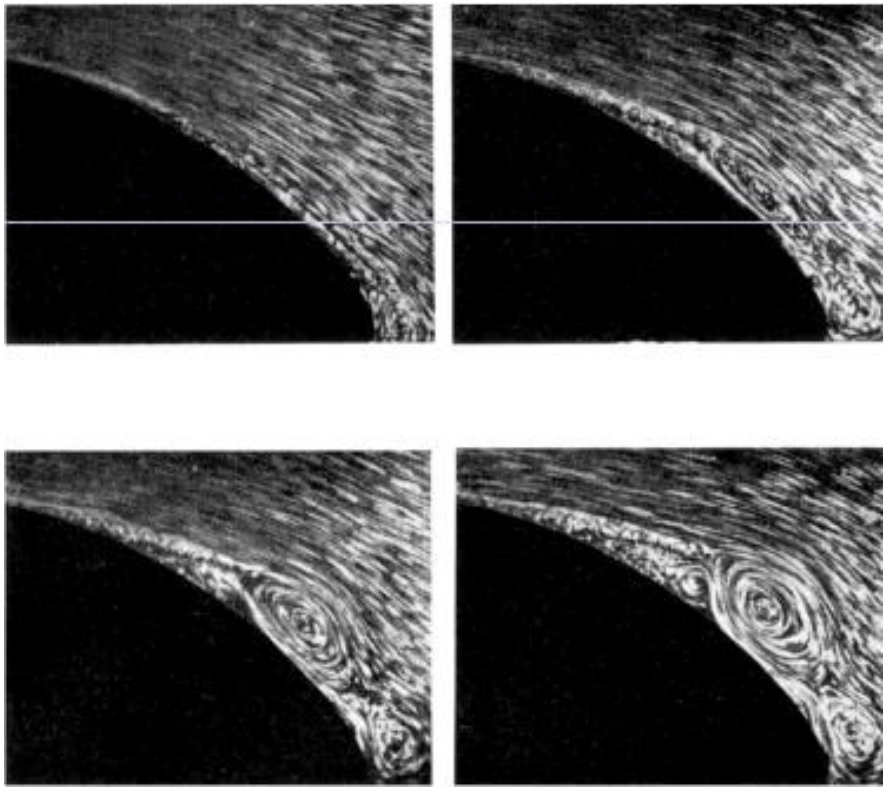

In the separation point A we have:

$$\left.\frac{\partial u}{\partial y}\right|_{y=0} = 0$$

Moreover, the viscous stress on the wall is zero:

$$\tau_w = 0$$

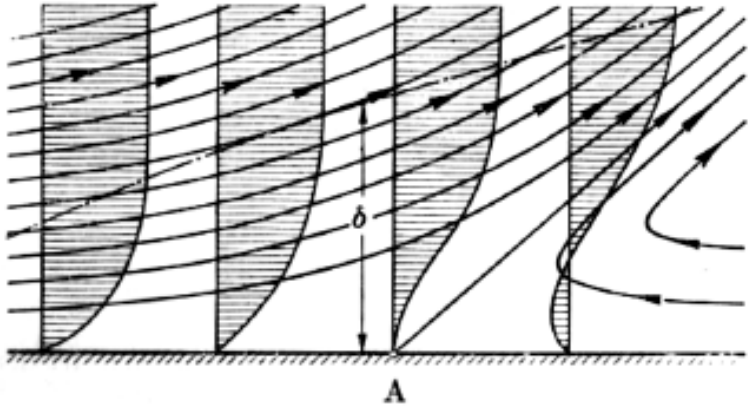

Separation may occur both in the laminar and turbulent boundary layer (in the turbulent one it occurs later, i.e. at the higher pressure gradients). Separation of the boundary layer has many negative consequences, it disturbs the operation of the fluid flow machinery and it reduces their efficiency. The fluid flow machinery should be designed in such a way that the separation of flow is avoided, at least at the design operation parameters of these machines.

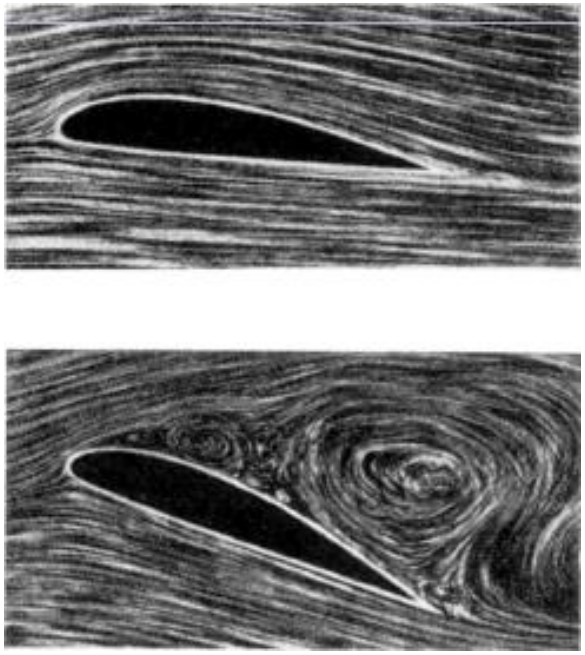

The separation bubble

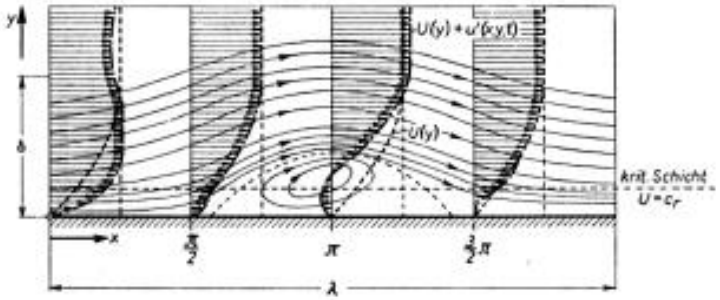

< Separation of the boundary layer on an airfoil at high angle of attack (lower picture)

Examples of the laminar and turbulent flows in the boundary layers and wakes

Chapter 20 – Boundary layers and wakes

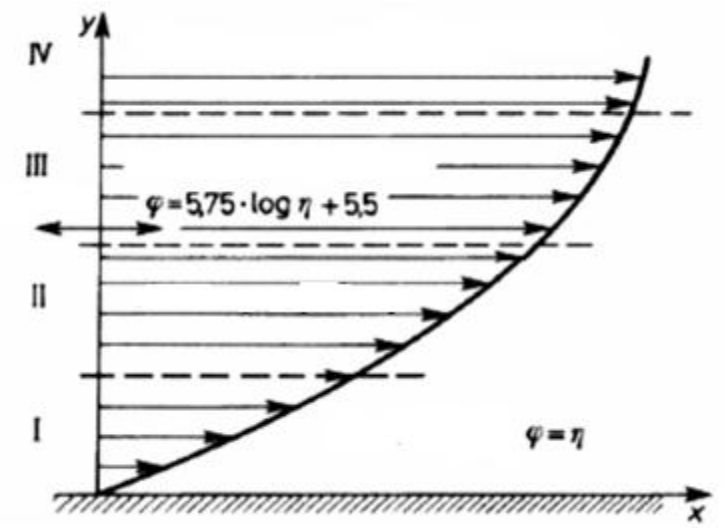

In the turbulent boundary layer several different regions may be distinguished, each with the different physical mechanisms governing the flow.

Generally, the boundary layer may be divided into the inner region of thickness about 0.2δ and the outer region (IV). In the outer region the inertia forces dominate the flow. The internal flow may be divided into the viscous sub-layer (I) of thicknessabout0.02δ, where the viscous forces and inertia forces are of the same order and where the viscous mechanism of momentum and energy transport is dominant, and the transitional (II) and„ logarithmic” (III) region, where the turbulent stresses and turbulent mechanism of mass, momentum and energy transport dominate the flow.

Due to the combined effect of the viscous and turbulent mechanisms of momentum transport the velocity profile in the turbulent layer is „fuller” than in the laminar layer.

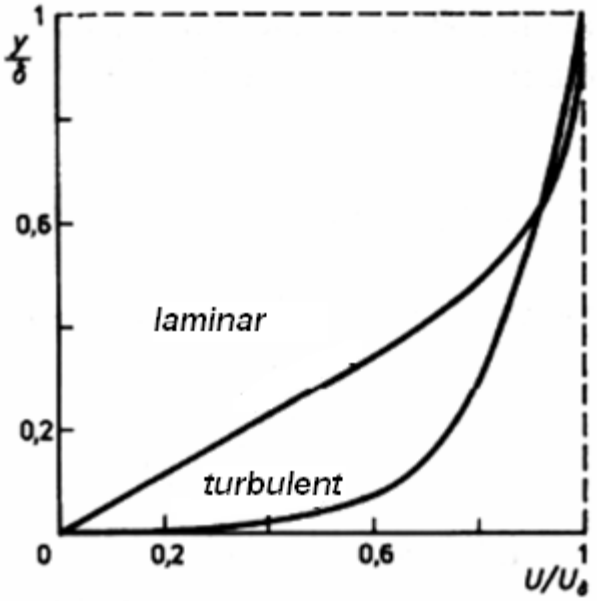

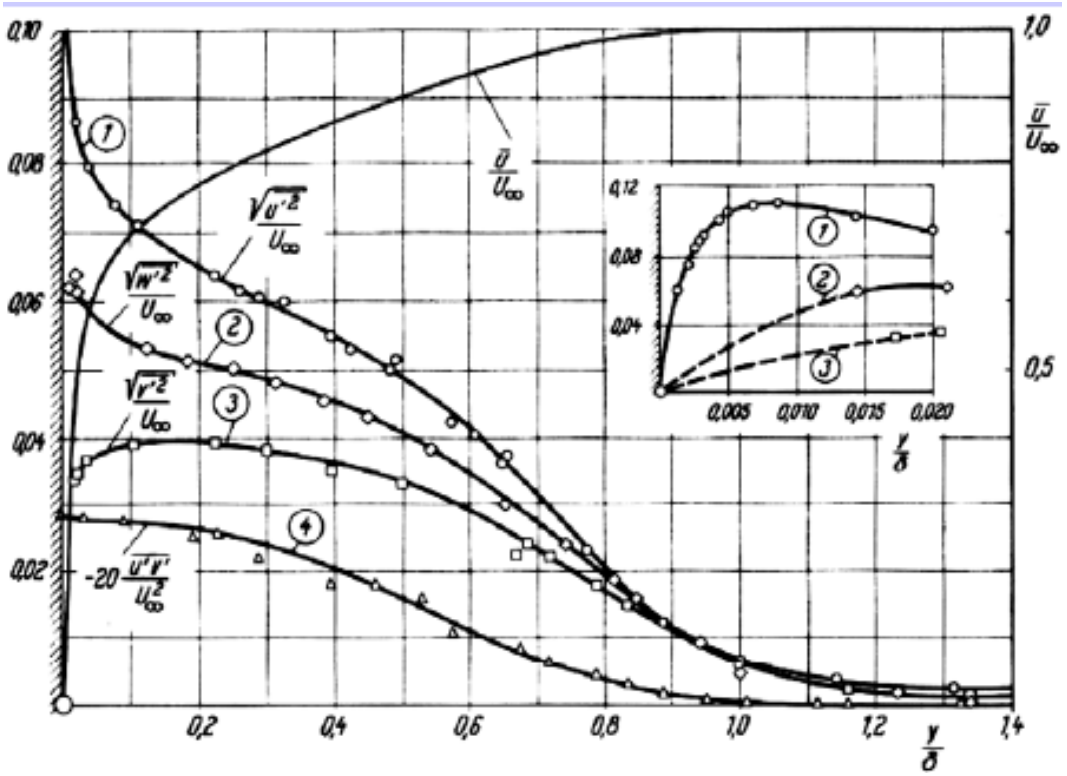

In the turbulent boundary layer strong, three-dimensional fluctuations of velocity occur. They attain maximum amplitudes near the wall i.e. in the region of high gradient of the mean velocity profile.

Some practically useful formulae have been developed using empirical-theoretical approach:

$$\delta_{turb} = \frac{0.37 \cdot L}{\sqrt[5]{\mathrm{Re}}}$$

$$C_{fturb} = \frac{0.074}{\sqrt[5]{\mathrm{Re}}}$$

for Reynolds numbers $5 \cdot 10^5 < \mathrm{Re} < 10^6$

$$C_{fturb} = \frac{0.455}{(\log \mathrm{Re})^{2.58}} - \frac{A}{\mathrm{Re}}$$

for $3 \cdot 10^5 < \mathrm{Re} < 10^9$

Where the constant A is determine do n the basis of the (upper) critical value of the Reynolds number according to the table:

Re	A
$3 \cdot 10^5$	1050
$5 \cdot 10^5$	1700
10^6	3300
$5 \cdot 10^5$	5700

The above formulae for the friction coefficient are valid for a smooth wall. In the turbulent flow this coefficient depends also on the wall surface roughness

The measure of the surface roughness is the mean roughness height k_s

From the point of view of the frictional drag, the ratio of the mean roughness height to the thickness of the viscous sub-layer in the turbulent boundary layer is important. If the roughness is totally contained in this sub-layer, then the roughness does not change the velocity profile in the boundary layer and does not affect the frictional drag – such a surface is called hydrodynamically smooth. When the roughness height exceeds the thickness of the viscous sub-layer, it changes the velocity profile in the boundary layer and increases the frictional drag.

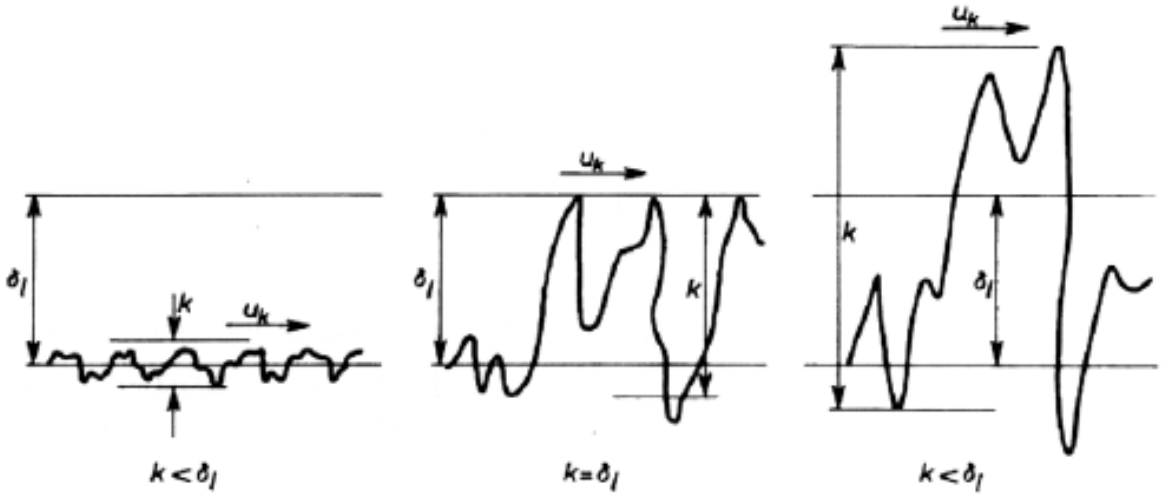

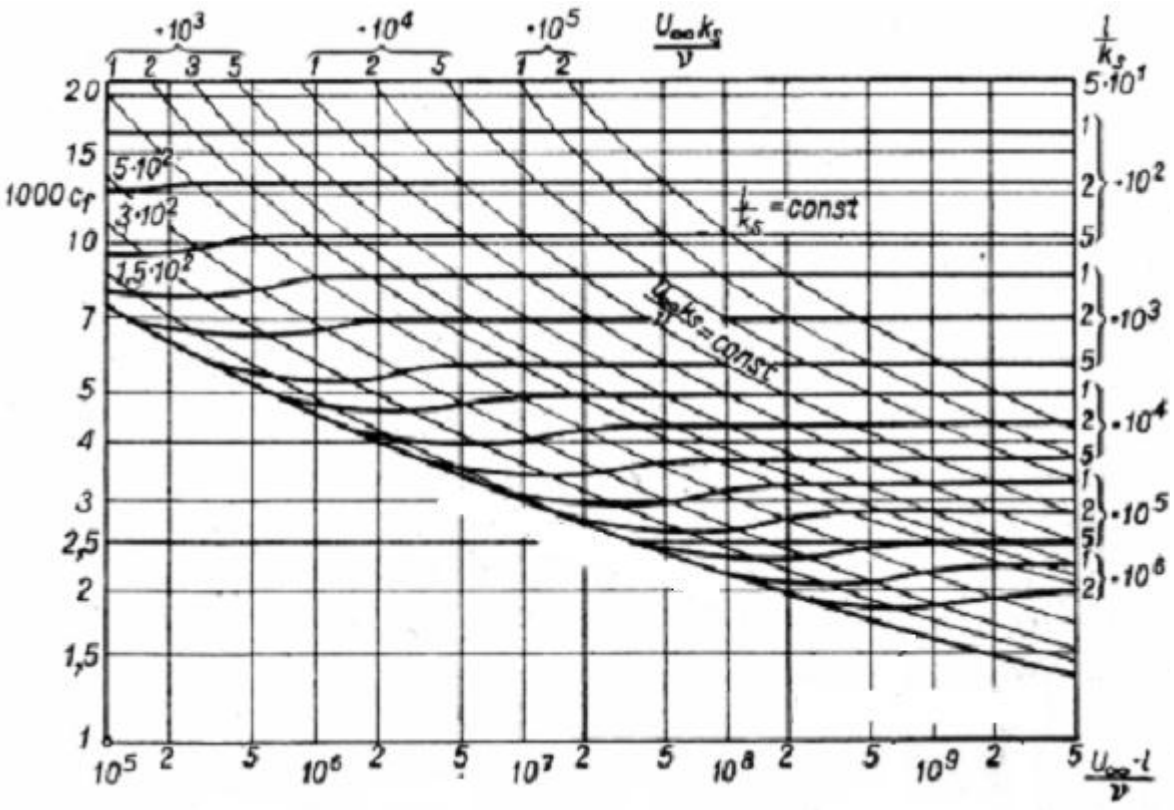

The diagram shows the dependence of the frictional drag coefficient on the inverted relative roughness (i.e. related to the characteristic linear dimension L). Reynolds numbers based on the roughness height are also marked in the diagram.

There are empirical relations, which enable determination of the frictional drag coefficient on a rough surface in the turbulent boundary layer, for example:

$$C_{fchrop} = C_{fturb} + \Delta C_f$$

where:

$$\Delta C_f = \left(1.89 + 1.62 \log \frac{l}{k_s}\right)^{-2.5} \qquad 10^2 < \frac{l}{k_s} < 10^6$$

Chapter 21 – Aerodynamics of the lifting foils

Lifting foils are important parts of many products of contemporary technology.

< Helicopters

Aircraft

Gliders

Sails >
< Keels and rudders
Hydrofoils
Ship propellers

Airscrews Water turbines >

Steam turbines >

Racing cars

< Pumps

Wind and water turbines >

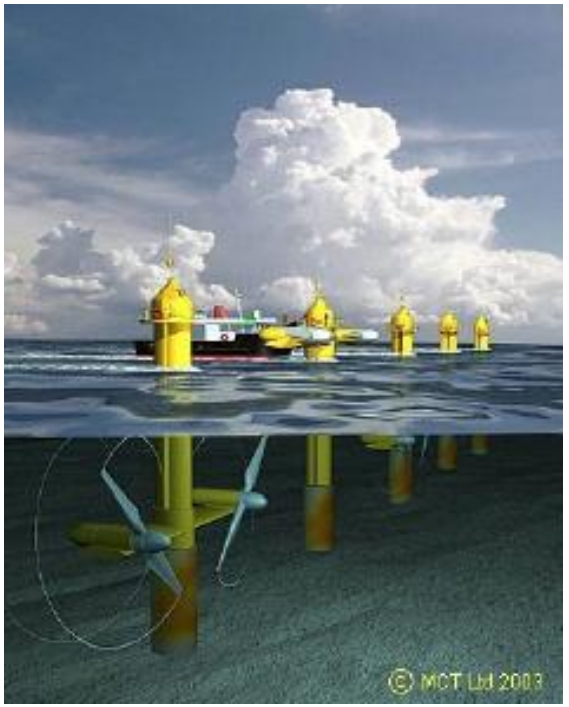

Nature always was and still is an inspiration for technology.

Aero- or hydrodynamic force is generated on any object placed in a flow.
This force may be decomposed into a component perpendicular to the flow velocity, called **the lift force** and a component parallel to the velocity of flow, called **the drag force**. **The lifting foils** are objects shaped in such a way that the **maximum lift force and minimum drag force** are attained. The characteristics of the foil depend to a large degree on the geometry of its cross-section perpendicular to the foil span, i.e. on the geometry of **the aerodynamic profile.**

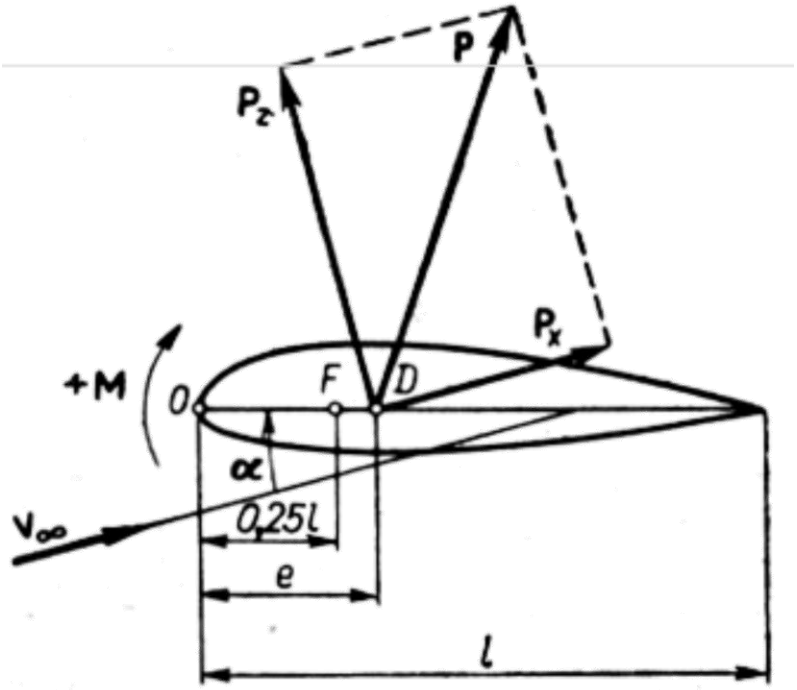

P – the resultant aerodynamic force

P_Z - the lift force

P_X - the drag force

M – the moment of the aerodynamic force

V_∞ - the flow velocity

α – the angle of attack

The point of action of the resultant aerodynamic force D changes its location with changing angle of attack, but as a rule it stays near the point F located at the distance 0,25 *l* from the leading edge, which is called the aerodynamic centre of the profile.

The real flow around a lifting foil may be modeled mathematically by means of a vortex:

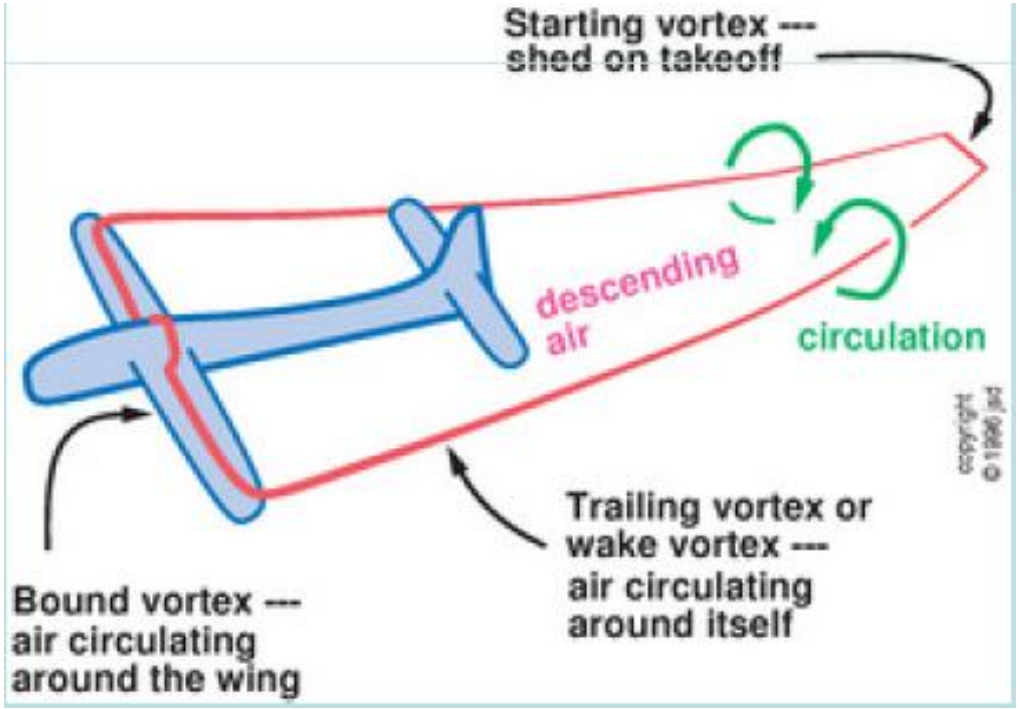

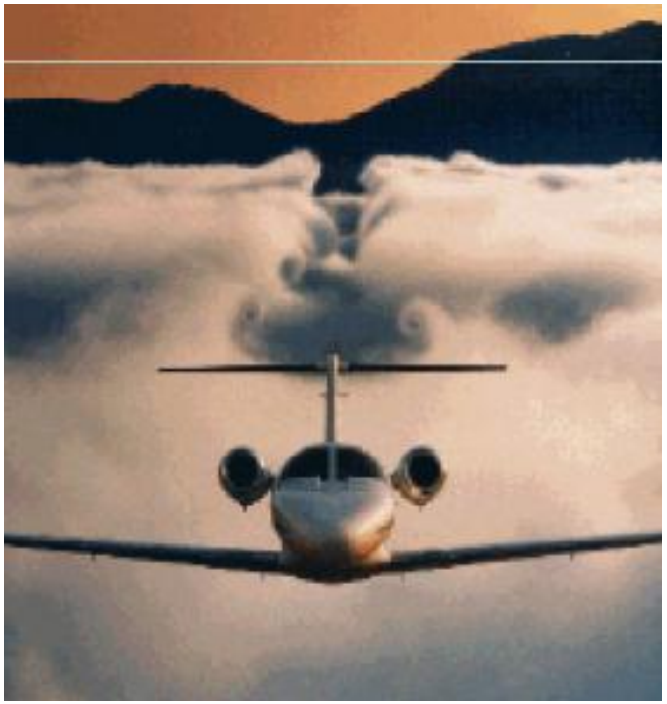

In order to produce the lift force on an airfoil it should be shaped in such a way that a **circulatory flow** is generated, i.e. the flow is asymmetrical with respect to the direction of the inflow velocity. Then on one side of the profile the velocity of flow increases and simultaneously pressure falls (this is so called **suction side**), and on the other side the velocity of flow decreases and simultaneously the pressure rises (this is so called **pressure side**). This pressure difference, acting on the profile generates the lift force. The circulatory flow is achieved either through cambering the airfoil or by setting it at a certain angle with respect to the flow velocity, called the angle of attack. In most cases the appropriate combination of both methods is used.

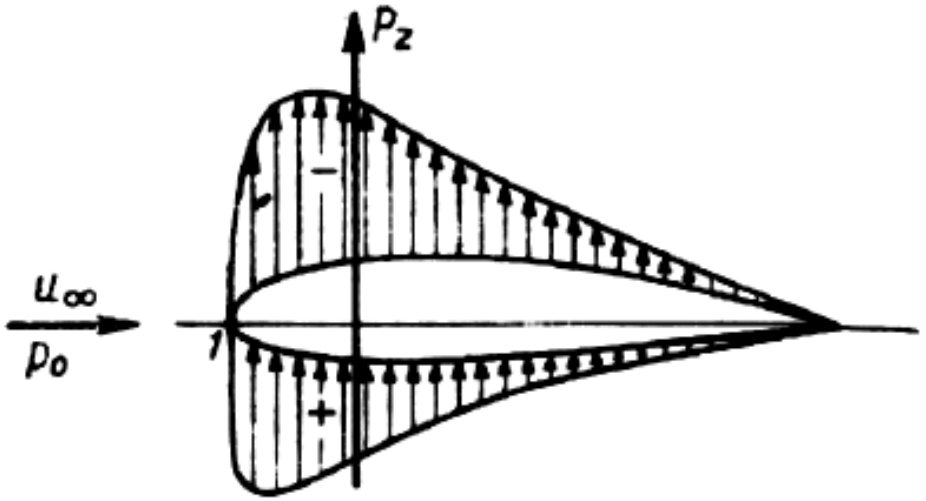

Geometry of the aerodynamic profiles

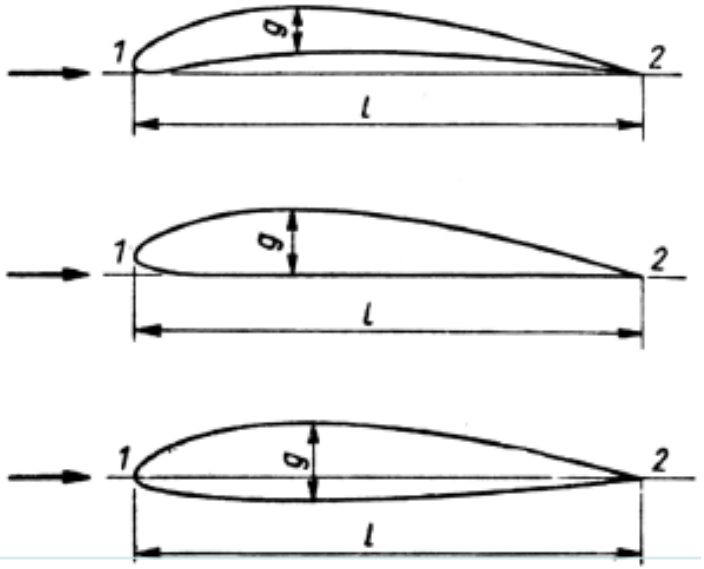

The profiles may be convex-concave (upper sketch), flat-convex (middle sketch), double-convex (lower sketch). Profile chord *l* is the distance between the two most distant points of the profile. Profile thickness *g* (or *d*) is the largest distance perpendicular to the chord limited by the profile contour.

The profile shape may be generated by an appropriate superposition of the symmetrical profile and the so called mean line.

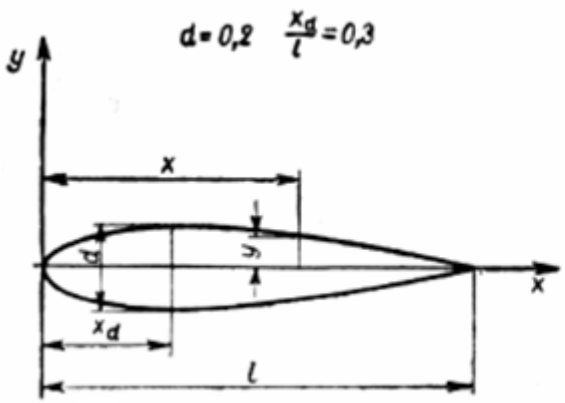

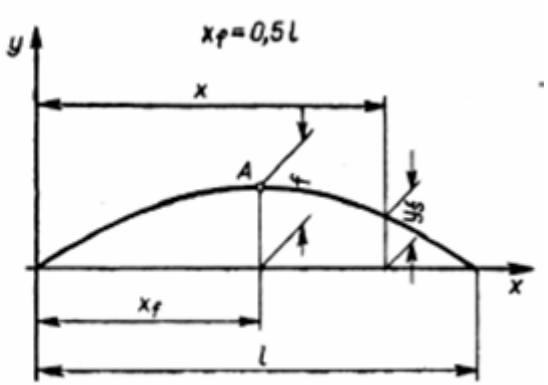

The form of the aerodynamic characteristics is reflecting the changing conditions of flow around the profile, resulting from the changes in the angle of attack. Moreover, it depends on the profile geometry, Reynolds number and Mach number.

At moderate angles of attack the lift force is a linear function of the angle of attack.

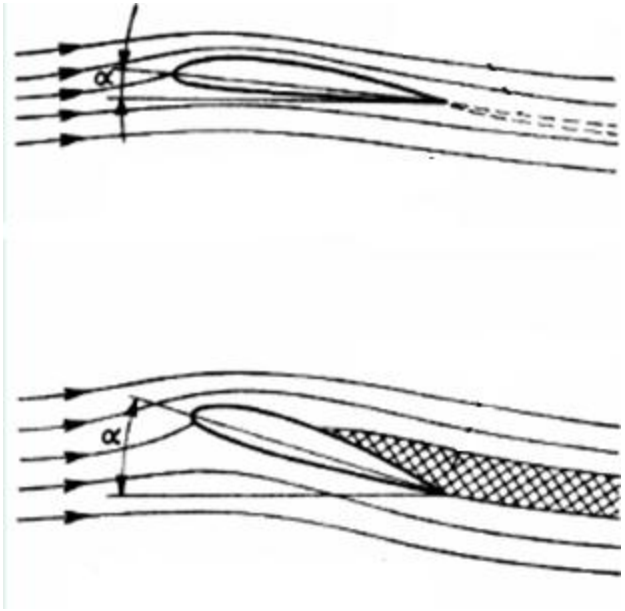

At high angles of attack the flow separation occurs and the lift force does not grow any further despite increasing angle of attack.

Some particular points of the aerodynamic characteristics are important:
Zero lift angle is proportional to the relative camber of the profile mean line:

$$\alpha_0 = k \cdot \frac{f}{l}$$

Maximum lift angle (critical angle of attack) corresponds to the occurrence of the developed flow separation on the suction side of the profile. For the profile NACA2418 we have:

$$\alpha_{kryt} = 17{,}8^0$$

Optimum angle of attack corresponds to the maximum efficiency of the profile. For the profile NACA2418 we have:

$$\alpha_{opt} = 2{,}6^0 \qquad \varepsilon = 20{,}6$$

Experimental testing and observations of air flow around different objects are performed in wind tunnels

- A large wind tunnel in Moscow (CAGI)
- External view of a wind tunnel
- Inside of the wind tunnel measuring section
- Six-parameter dynamometer for measuring forces on a model

Different experiments performed in wind tunnels

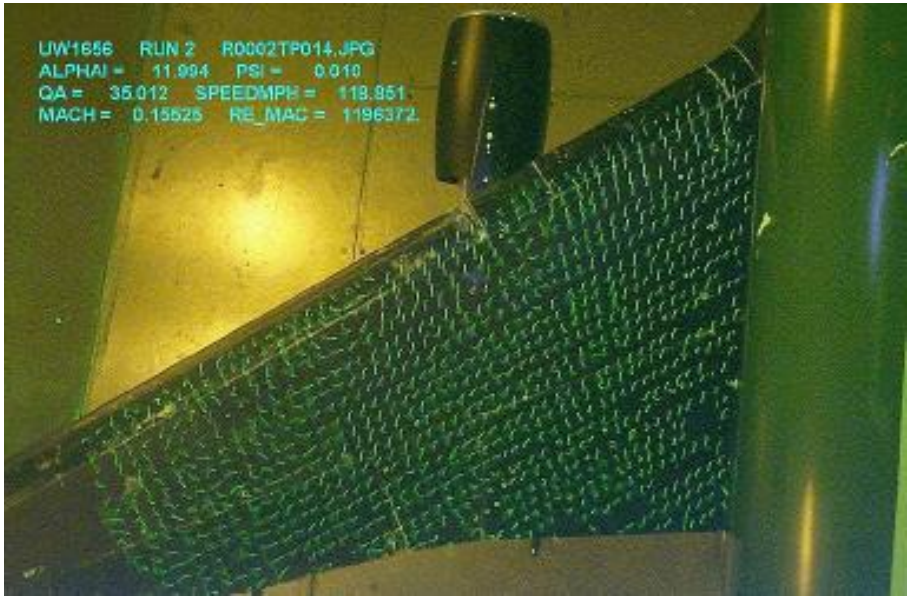

Chapter 22: Cavitation – Physical basics – Hydrodynamic consequences

Definition of cavitation

Cavitation is the phenomenon of the dynamic growth and decay of vapour-gas bubbles in the liquid, generated by the changes in pressure at (almost) constant temperature.

The process of cavitation is controlled by:

- diffusion/degassing
- evaporation/condensation
- inertia of the fluid
- surface tension
- adhesion
- viscosity of the fluid

Cavitation may occur in:
• liquid gases – rocket fuel,
• liquid metals – coolants in nuclear reactors,
• natural liquids – working fluids in hydraulic machines (e.g. fuel in a Diesel engine),
• blood – in the flow through an artificial heart valve.

The parameter describing similarity of the cavitation phenomena is the cavitation number (or index) σ

$$\sigma = \frac{p - p_v}{\frac{1}{2}\rho U^2}$$

where: p – pressure in the given point of flow
p_v - critical vapour pressure, about 2000 [Pa]
U – velocity of flow
ρ – density of liquid
The simplified condition of cavitation inception has the form:

$$C_p = \frac{p_\infty - p}{\frac{1}{2}\rho U^2} \geq \sigma = \frac{p_\infty - p_v}{\frac{1}{2}\rho U^2} \qquad p \leq p_v$$

where: p_∞ **- pressure „far in front" of the object**

***p* – pressure in the considered point on the object**

Approximate assessment of the cavitation inception and its extent in different operating conditions of a profile

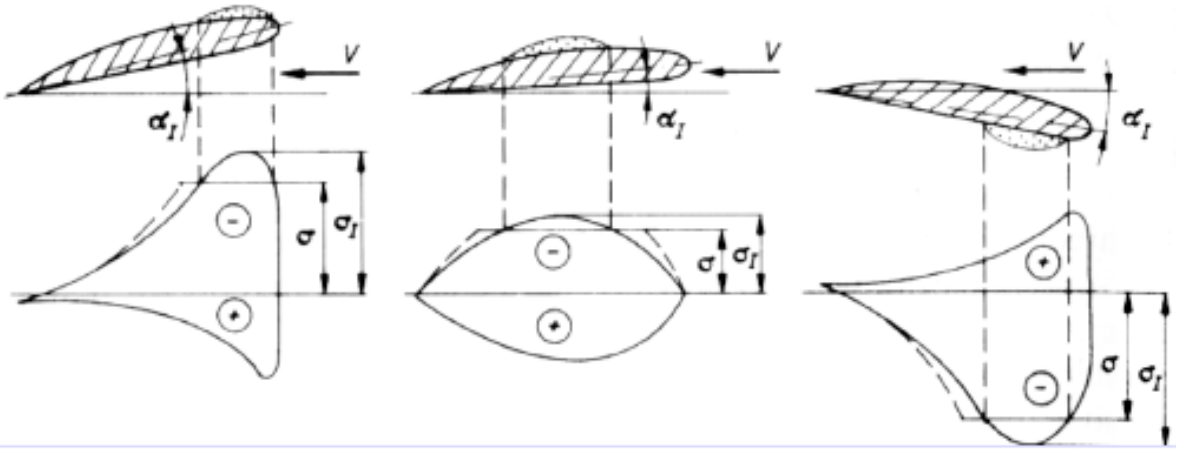

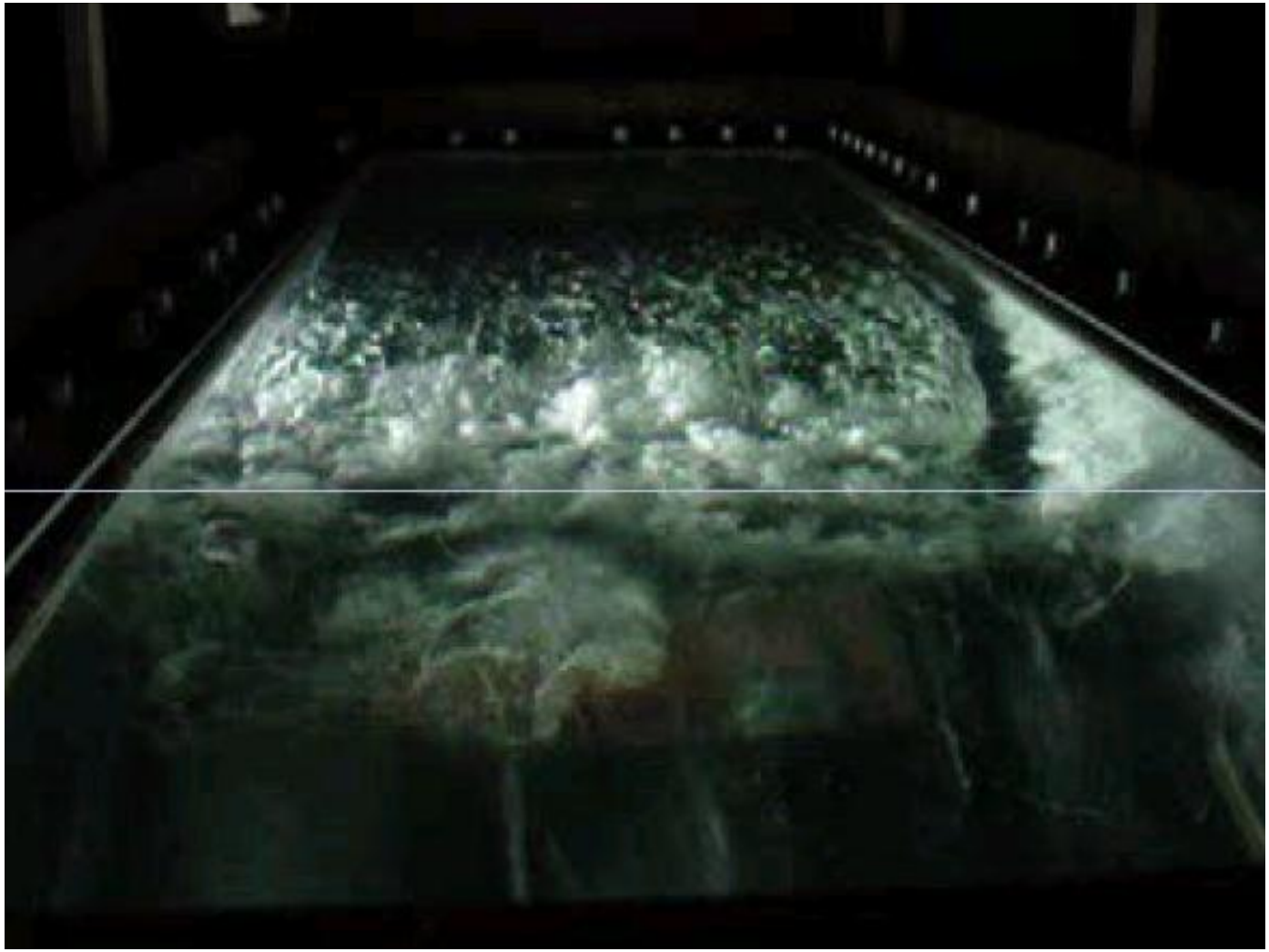

Inception of cavitation

Inception of cavitation occurs when the microbubbles naturally contained in a liquid are destabilised

$$p_e = p_v + p_g - \frac{2\sigma}{R}$$

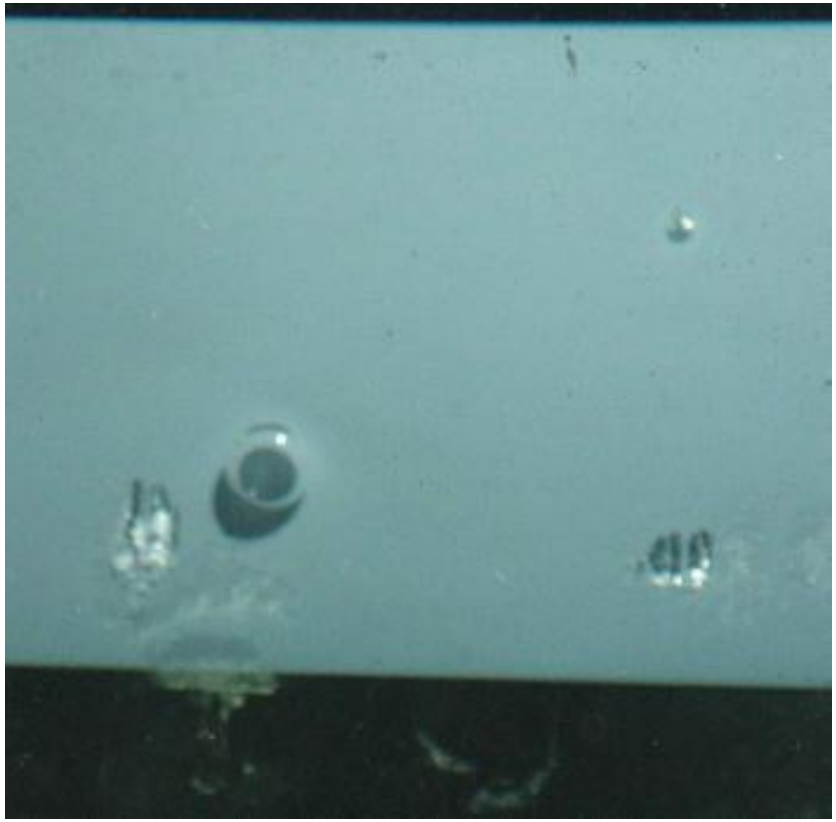

The history of growth and decay of the cavitation bubble

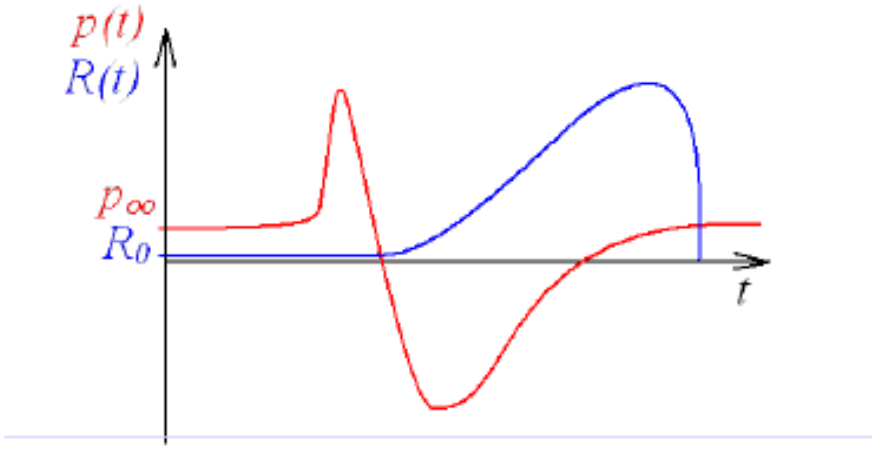

Rayleigh-Plesset equation

$$R\frac{d^2R}{dt^2}+\frac{3}{2}\left(\frac{dR}{dt}\right)^2+4\frac{\mu}{\rho R}\frac{dR}{dt}=-\frac{p_\infty+\frac{2A}{R}-p_v-p_g}{\rho}$$

R – radius of the bubble
A – surface tension of the liquid

Comparison of the calculated and observed cavitation extent

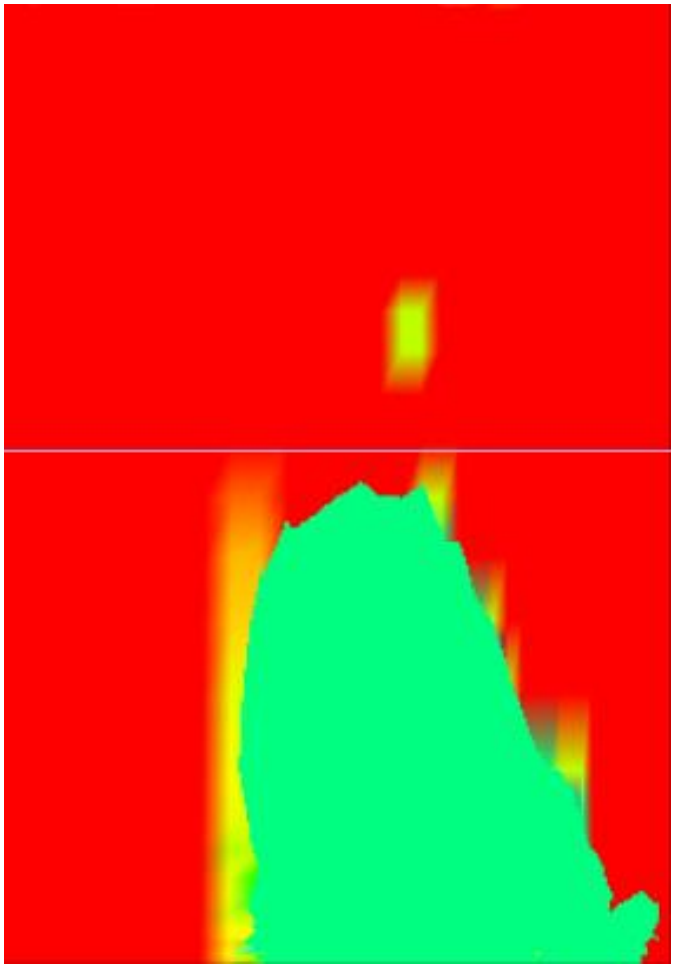

Forms of cavitation

High tension in fluid, acting sufficiently long to destabilize most of the micro-bubbles

Sheet cavitation

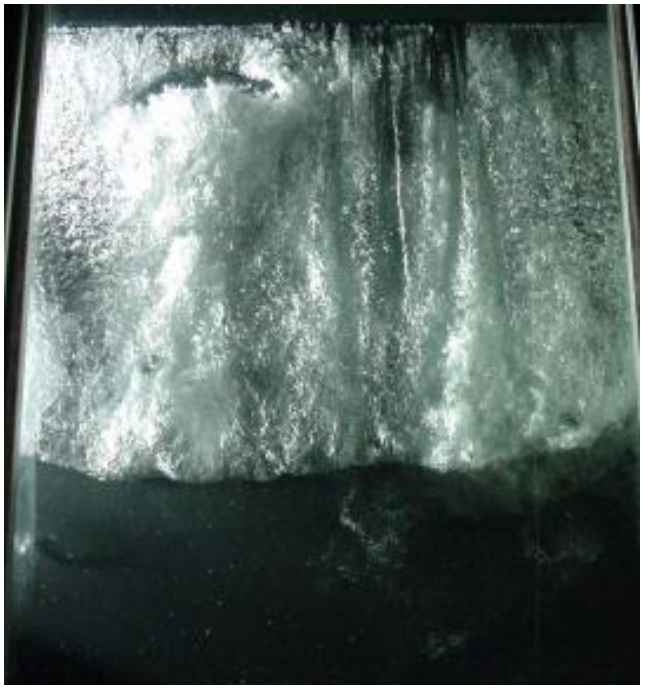

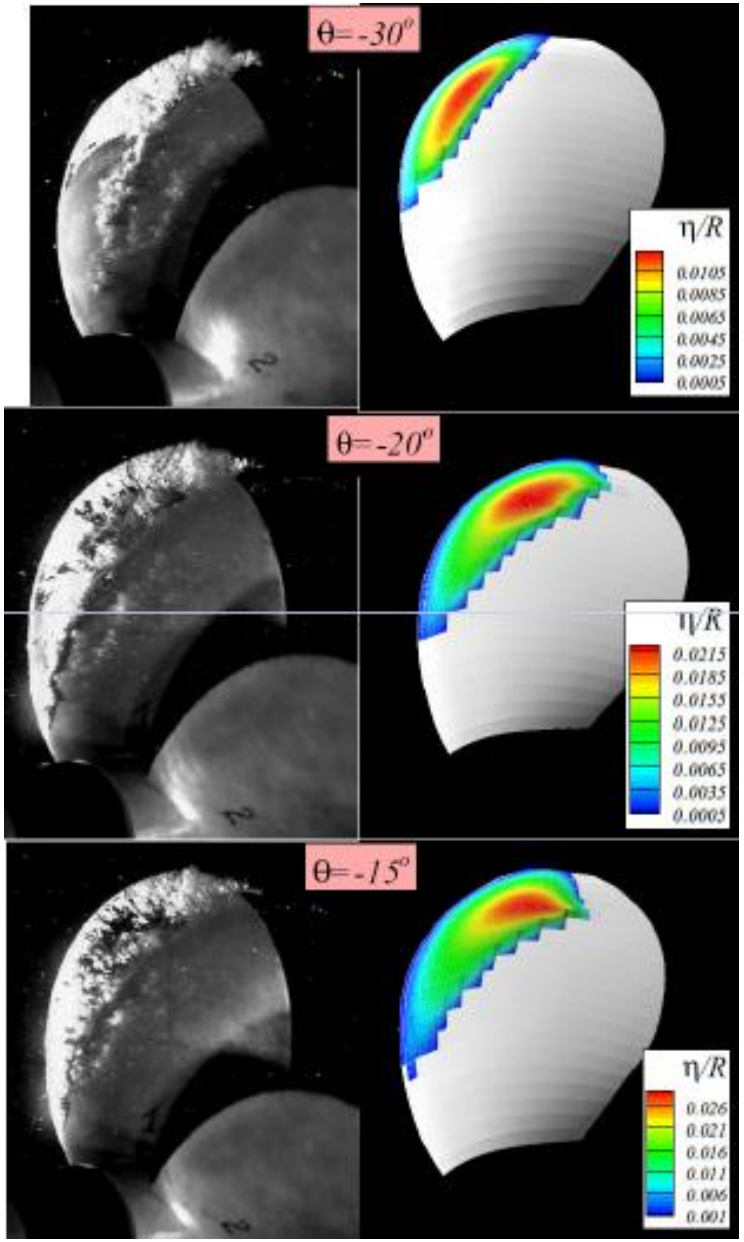

Computational determination of sheet cavitation on the ship propeller blade, compared with the experimental observation

Forms of cavitation

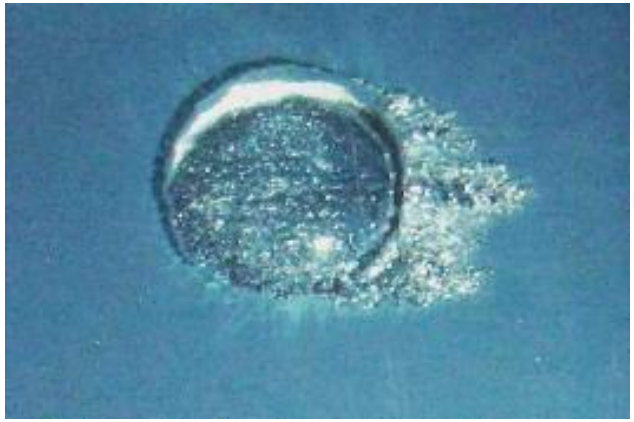

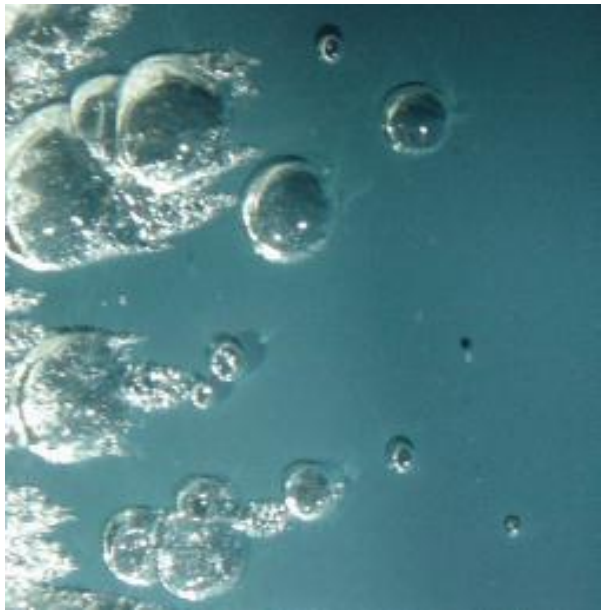

Bubble cavitation
Low tension in the liquid, destabilising only the largest micro-bubbles, which are few and far between

Forms of cavitation

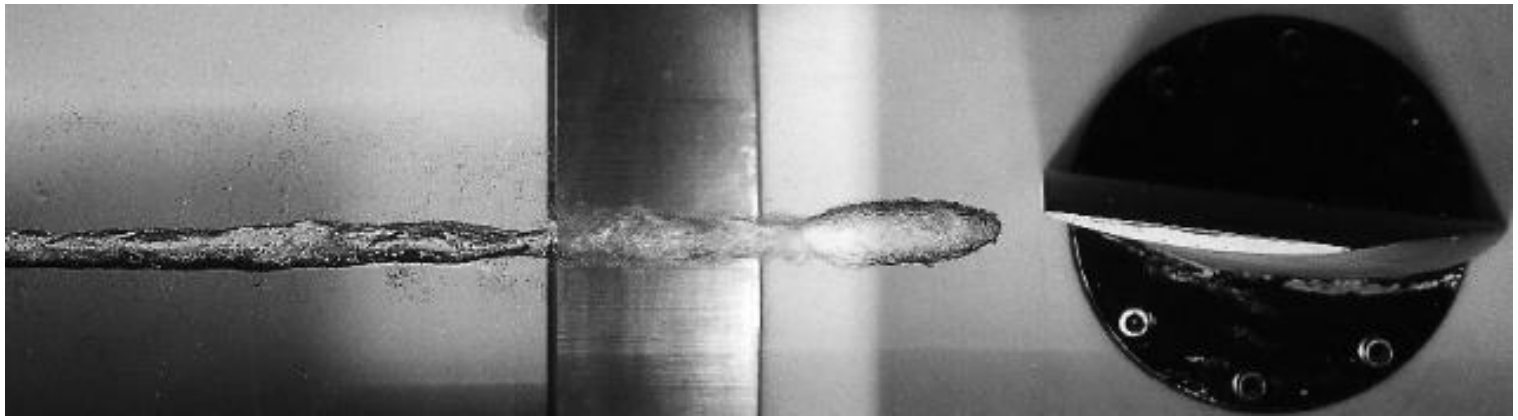

Vortex cavitation

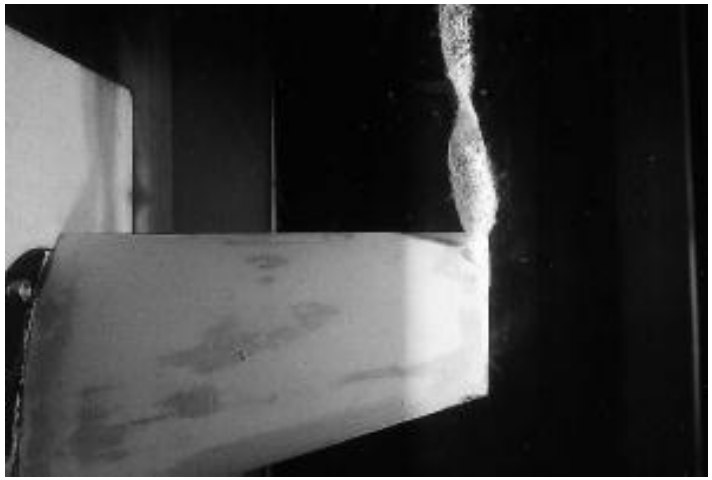

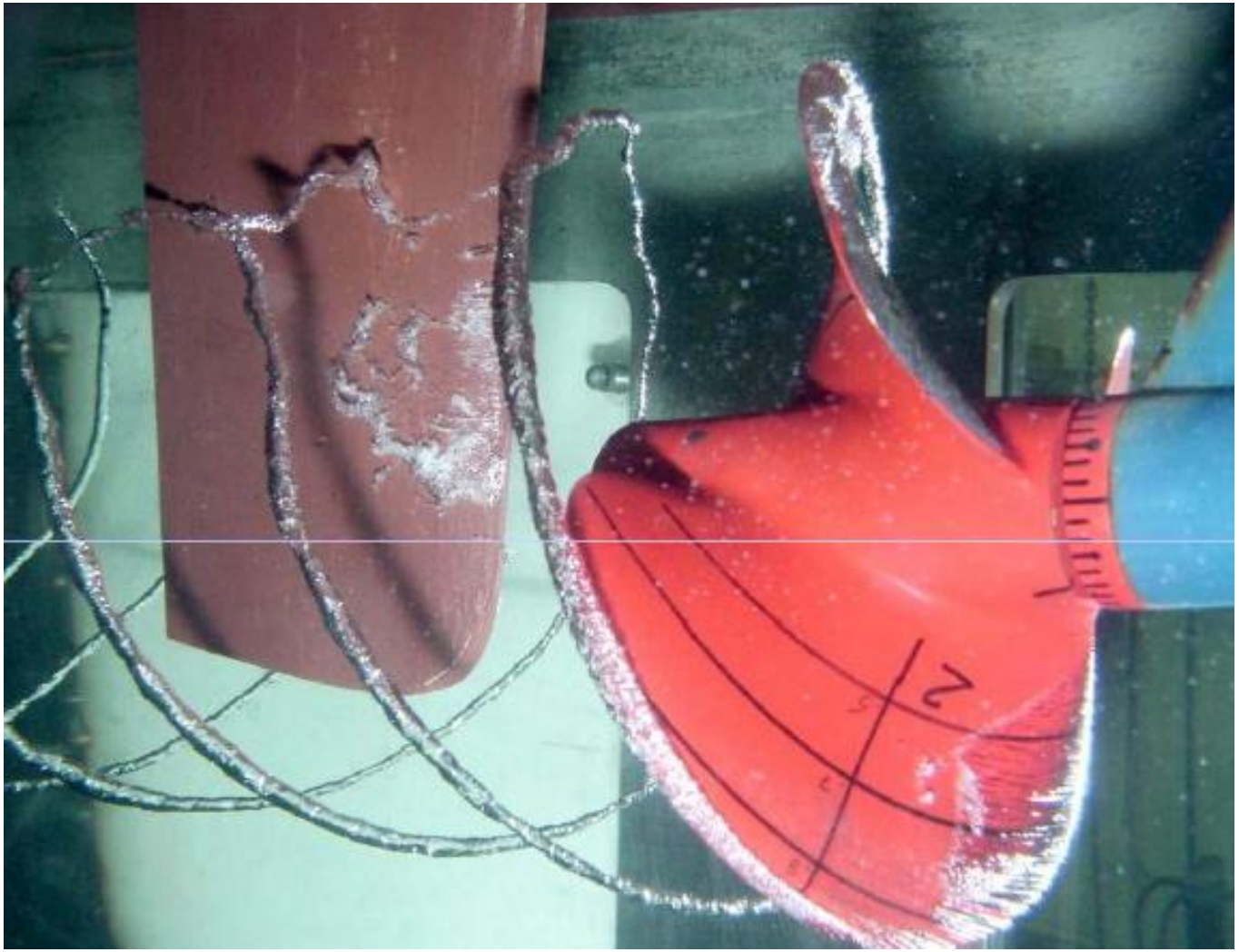

The cavitating tip vortex on a ship propeller deformed by the rudder interaction

Transient forms of cavitation

Cloud cavitation
Increase of pressure in the fluid leads to the transient forms of cavitation

Consequences of cavitation

- reduction in efficiency of the fluid flow machinery
- cavitation erosion
- noise and vibration

Cavitation erosion

The process of decline of a cavitation bubble near a solid wall

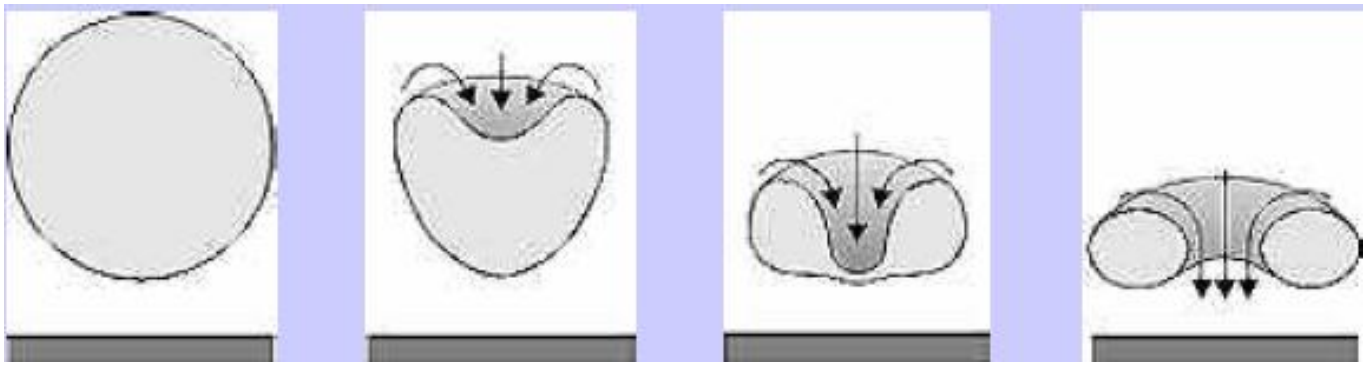

Erosion on the ship propeller blades

Noise

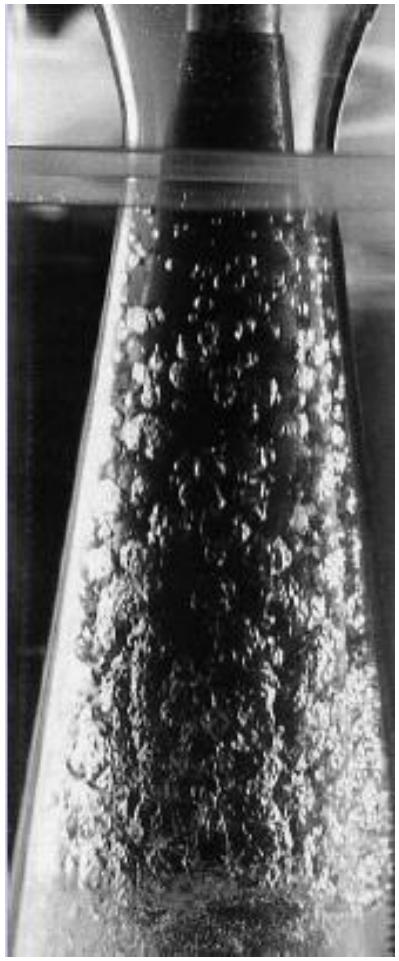

$$R\ddot{R} + \frac{3}{2}\dot{R}^2 + \frac{2\sigma}{\rho R} + 4\mu\frac{\dot{R}}{\rho R} = F(t)$$

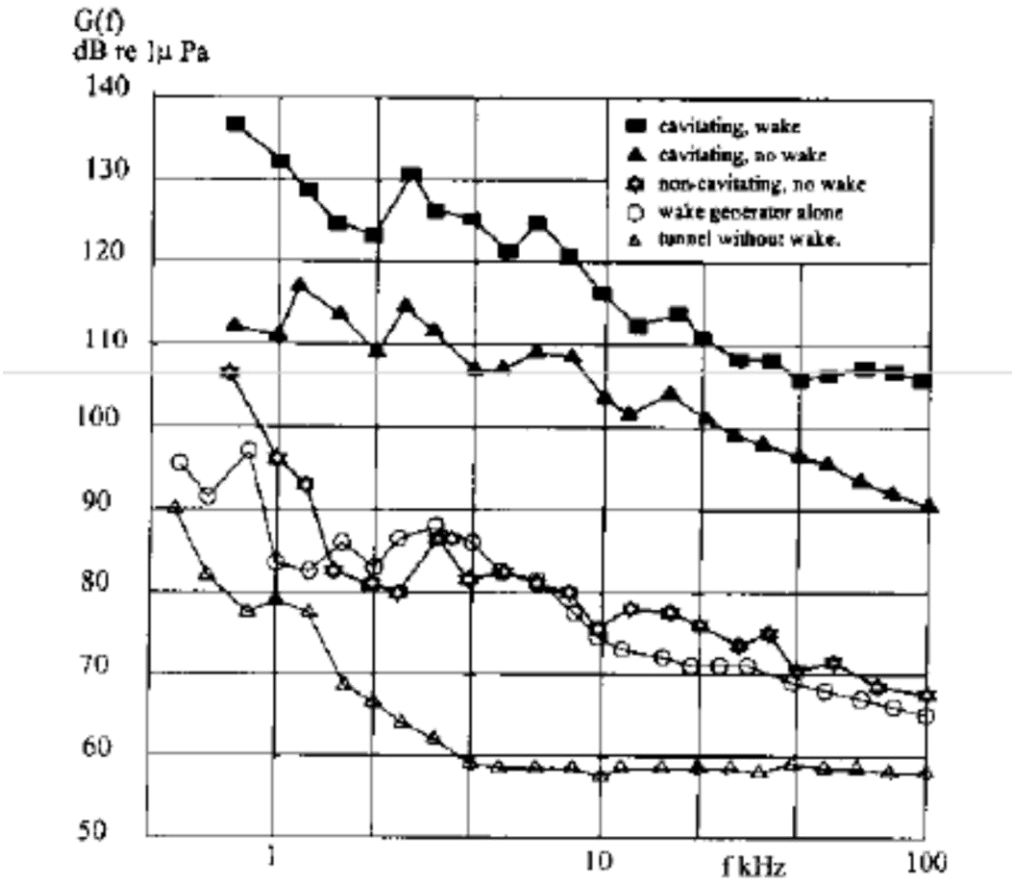

Spectrum of noise generated by a ship propeller

Conclusion

• All machines and devices in which liquid is the working fluid are susceptible to cavitation.

• Cavitation results in serious negative consequences, which may adversely affect the operation and may lead to the damage these machines and devices.

• Limitation or elimination of cavitation and its negative consequences requires special, complicated methods for design of these machines and devices, using modern experimental techniques and the most advanced theoretical and numerical methods.